MODELING RESONANCE INTERFERENCE BY 0-D SLOWING-DOWN SOLUTION WITH EMBEDDED SELF-SHIELDING METHOD

Yuxuan Liu and William Martin
Department of Nuclear Engineering and Radiological Sciences
University of Michigan
2355 Bonisteel Blvd., Ann Arbor, MI, 48109
yuxuanl@umich.edu; wrm@umich.edu

Kang-Seog Kim and Mark Williams
Oak Ridge National Laboratory
One Bethel Valley Road, P.O. Box 2008, Oak Ridge, TN 37831-6172, USA
kimk1@ornl.gov; williamsml@ornl.gov

ABSTRACT

The resonance integral table based methods employing conventional multigroup structure for the resonance self-shielding calculation have a common difficulty on treating the resonance interference. The problem arises due to the lack of sufficient energy dependence of the resonance cross sections when the calculation is performed in the multigroup structure. To address this, a resonance interference factor model has been proposed to account for the interference effect by comparing the interfered and non-interfered effective cross sections obtained from 0-D homogeneous slowing-down solutions by continuous-energy cross sections. A rigorous homogeneous slowing-down solver is developed with two important features for reducing the calculation time and memory requirement for practical applications. The embedded self-shielding method (ESSM) is chosen as the multigroup resonance self-shielding solver as an integral component of the interference method. The interference method is implemented in the DeCART transport code. Verification results show that the code system provides more accurate effective cross sections and multiplication factors than the conventional interference method for UO2 and MOX fuel cases. The additional computing time and memory for the interference correction is acceptable for the test problems including a depletion case with 87 isotopes in the fuel region.

Key Words: Resonance interference, RIF model, homogeneous slowing down, ESSM

1. INTRODUCTION

When deterministic neutron transport methods are applied to lattice or whole-core problems, the multigroup approximation is typically applied in the energy domain. Evaluation of multigroup cross sections is a crucial challenge due to the complicated behavior of resonance cross sections. There are in general two ways of performing the resonance self-shielding calculation. The best approach for assuring accuracy in the energy domain is to solve the slowing-down equations for the problem of interest. The continuous-energy (CE) cross sections are needed to resolve the resonance behavior. Because of the limited computational resources, slowing-down codes such as CENTRM [1] and RMET21 [2] usually assume 1-D cylindrical geometry that has been converted from the square pin cell using the Wigner-Seitz approximation. The assumption of 1-D cylindrical geometry does not account for the inter-pin spatial self-shielding effects in the actual

CASL-U-2015-0007-000

reactor geometry. The second approach utilizes pre-computed resonance integral (RI) tables, which are established by the slowing-down solution over a range of background cross sections. Based on the equivalence theory [3], different methods can be derived in order to determine the equivalence cross sections to account for spatial self-shielding. The Bondarenko background cross section method [4] is the conventional method incorporating Dancoff factors to account for the spatial self-shielding. The subgroup method [5] is another RI table based method where the RI tables are usually converted to a set of subgroup levels and weights so that the equivalence cross sections are subgroup-level dependent. Recently another promising RI table based method, the iterative self-shielding method [6] [7] was proposed by Korea Atomic Energy Research Institute (KAERI) and Oak Ridge National Laboratory (ORNL). ORNL entitled it Embedded Self-Shielding Method (ESSM) because compared to the conventional Bondarenko method in which the Dancoff factors should be approximated or evaluated outside the transport calculation, ESSM provides tighter coupling between the neutron transport and self-shielding calculations, so that the heterogeneous self-shielding effects are consistent with the multigroup transport calculations of the whole system.

However, RI table based methods such as subgroup and ESSM have difficulty of treating the interference effect among resonance isotopes. This is due to the fact that the RI tables are generated at different temperatures and dilutions for each single resonance isotope by solving the slowing-down equation with CE cross sections. The interference effect is neglected at this step and is assumed to be treated at the multigroup level, e.g., by Bondarenko iteration described in the WIMS code [8]. As shown in Williams's early research [9], the corrections for interference effect in the multigroup framework cannot account for resonance overlap in a mixture of resonance isotopes.

Methods have been developed in attempt to capture the interference effect by adding parameters to the RI tables. Ref. [10] shows a possibility of including the density ratio of two resonance isotopes in the RI table to allow an estimate of the interference effect of two isotopes using a direct RI table method such as ESSM. Ref. [11] also provides a way by introducing isotopic density ratios which are parameterized through the subgroup weights for the subgroup method. However, for MOX fuel or depleted fuel in which more than two resonance isotopes have notable impact on the spectra, it is difficult to construct and interpolate within a large RI table with multiple parameters accounting for the density ratios among dozens of resonance isotopes. In addition to the table complexity, the method depends on expert judgment regarding the dominant resonance isotopes, which complicates its extension to new fuel types such as thorium-based fuel.

An approach that addressed these issues was the Resonance Interference Factor (RIF) method [9]. In the RIF method, two sets of self-shielded multigroup cross sections are created for every resonance isotope in the fuel. One set is created with a flux spectrum generated by isolating a single resonance isotope from all other absorbers in the fuel mixture. The other set is created with a flux spectrum generated by considering the entire fuel mixture of resonance isotopes. Then for each resonance isotope, the two sets of self-shielded multigroup cross sections are compared and interference factors can be obtained to account for the interference effect of a concerning problem. The RIF model is developed in the lattice physics code LANCER02 [12] and the results show that RIF correction can properly account for resonance interference.

Furthermore, Kim and Williams improved the RIF model recently by using the spectra from the rigorous slowing-down solutions, which are able to capture the interference effect accurately in the energy domain [13-14].

We have incorporated an alternative CE slowing-down solver into the improved RIF model [13-14] and have verified its results for realistic reactor configurations. Two advantage features of the new slowing-down solver include: (1) decreased memory demand by using a problem-dependent energy mesh from CENTRM but simplified for a homogeneous medium, instead of an equal-lethargy mesh, and (2) improved efficiency by interpolating self-shielded cross sections for the single resonance isotopes from pre-calculated homogeneous RI tables rather than being solved on the fly. These two features allow the new RIF method to run on a current PC and does not significantly increase the computational time even for the depleted cases with dozens of resonance isotopes in the fuel. The new RIF method includes the ESSM as the multigroup resonance self-shielding solver and has been incorporated into the DeCART transport code [15]. The results obtained with the modified version of DeCART are in good agreement with MCNP solutions with only modest increases in execution time and memory demand.

2. Methodology

2.1. ESSM and RIF Model

ESSM is fundamentally a variation of the extensively used Bondarenko method. It accurately evaluates the equivalence cross section by performing iterations between a fixed-source transport problem and calculation of the self-shielded cross sections for the geometry being analyzed. The subgroup approach also uses fixed-source transport solutions to evaluate the subgroup-level dependent equivalence cross sections. The advantage of ESSM is that it does not require complicated generation of subgroup levels and weights. The implementation of ESSM described in this paper is slightly different from that described in Ref. [6][7].

Our goal is to evaluate multigroup self-shielded cross sections,

$$\sigma_{x,g} = \int_{\Delta u_g} \sigma_x(u)\phi(u)du \Big/ \int_{\Delta u_g} \phi(u)du \tag{1}$$

where x is a specific reaction channel and g is the index of an energy (lethargy) group. The weighting flux in Eq. (1) is the solution of the neutron slowing-down equation for a specific configuration. The slowing-down equation in a homogeneous medium is given as

$$\sum_i \Sigma_{t,i}(u)\phi(u) = \sum_i \int_{u-\varepsilon_i}^{u} \Sigma_{s,i}(u')\phi(u')\frac{e^{u'-u}}{1-\alpha_i}du' \tag{2}$$

where i is summed over all isotopes of the material, and ε_i is the maximum lethargy gain when a neutron scatters off isotope i. Three major assumptions have been made in this equation for the resolved resonance energy range: (1) the scattering source includes only s-wave elastic reactions; (2) up-scattering is neglected; and (3) the direct fission source is neglected. In order to decouple

CASL-U-2015-0007-000

the lethargy dependence in the scattering source from lethargy $u-\varepsilon_i$ to u, the Intermediate Resonance (IR) approximation [16] is employed to obtain:

$$\sum_i \Sigma_{t,i}(u)\phi(u) = \sum_i \lambda_i \Sigma_{p,i} + \sum_i (1-\lambda_i)\Sigma_{s,i}(u)\phi(u) \tag{3}$$

A more common form of the flux for self-shielding calculations can be achieved by neglecting the resonance scattering term $\lambda_i \Sigma_{RS,i}(u)$ (note $\Sigma_{s,i}(u) = \Sigma_{RS,i}(u) + \Sigma_{p,i}$) in the second term of the right-hand side, such that the flux is primarily a function of the absorption and potential scattering cross sections:

$$\phi(u) = \frac{\sum_i \lambda_i \Sigma_{p,i}}{\sum_i \Sigma_{a,i}(u) + \sum_i \lambda_i \Sigma_{p,i}} \tag{4}$$

The equivalence theory [3] correlates the solution of the homogeneous resonance problem with the heterogeneous problem by introducing the equivalence cross section Σ_e:

$$\phi_{het}(u) = \frac{\sum_i \lambda_i \Sigma_{p,i} + \Sigma_e}{\sum_i \Sigma_{a,i}(u) + \sum_i \lambda_i \Sigma_{p,i} + \Sigma_e} = \frac{\Sigma_b}{\sum_i \Sigma_{a,i}(u) + \Sigma_b} \tag{5}$$

By introducing Eq. (5) into Eq. (1), the effective cross section is a function of the background cross section Σ_b, so a table of effective cross section (or RI) can be built through various background levels. It should be mentioned that RI tables are for a single resonance isotope, therefore, no resonance interference is taken into account at this step.

ESSM directly uses these RI tables for cross section interpolation. An initial set of effective absorption cross sections can be obtained by assuming $\Sigma_e = 0$ for the fixed source problem (FSP)

$$\Omega \nabla \varphi_g(r,\Omega) + \left[\sum_i \Sigma_{a,i,g}(r) + \sum_i \lambda_i \Sigma_{p,i,g}(r) \right] \varphi_g(r,\Omega) = \frac{1}{4\pi} \sum_i \lambda_i \Sigma_{p,i,g}(r) \tag{6}$$

By solving the FSP, updated equivalence cross sections Σ_e are obtained from the correlation of flux and equivalence cross section in Eq. (5), which allows a new set of effective cross sections to be interpolated through the RI tables and hence a new FSP can be formulated. The iterations continue until the equivalence cross sections Σ_e converge.

Once the equivalence cross sections are properly determined, the RIF model comes into play. The slowing-down equation for an equivalent homogeneous problem relative to the problem of interest can be formulated by adding the equivalence cross section on both side of Eq. (2)

CASL-U-2015-0007-000

$$\left(\sum_i \Sigma_{t,i}(u) + \Sigma_{e,G}\right)\phi(u) = \sum_i \int_{u-\varepsilon_i}^{u} \Sigma_{s,i}(u')\phi(u')\frac{e^{u'-u}}{1-\alpha_i}du' + \Sigma_{e,G} \tag{7}$$

Noting the equivalence cross section is evaluated per coarse group from ESSM, approximation is made by using the average value instead of the one with continuous lethargy dependency. The RIF calculation involves solving Eq. (7) twice, once for the mixture of all isotopes, the other for a single resonance isotope with other isotopes treated as background isotopes $\left(\sigma_t(u) = \sigma_s(u) = \sigma_p\right)$. The two spectra are then used to collapse the effective cross sections and the ratio of the two effective cross sections for each resonance isotope *i* at each reaction channel *x* is defined as the resonance interference factor (RIF),

$$RIF_{x,i,g} = \frac{\sigma_{x,i,g}^{\text{int}erfered}}{\sigma_{x,i,g}^{non-\text{int}erfered}} \tag{8}$$

The last step is to modify the ESSM analysis by correcting the non-interfered effective cross section to account for interference.

2.2. Mesh Scheme for Homogeneous Slowing-down Solver

Eq. (7) can be solved by either an equal-lethargy mesh or a problem-dependent mesh. The number of energy points affects the computational time and memory requirement of the solver, which is a primary concern of the interference model because the conventional method of Bondarenko iteration is extremely fast and requires no additional memory. Methods for treating the scattering source with an equal-lethargy mesh can be found in a few references such as Ref. [2]. In this section, we adapt the CENTRM methodology and formulate a simplified problem-dependent mesh scheme specially for the homogeneous calculations.

Compared with the fixed energy points of an equal-lethargy mesh, the problem-dependent mesh has a more flexible mesh size which is primarily dependent on the dependence of the macroscopic total cross section of the material versus energy. To construct an optimized problem-dependent mesh, the first step is to construct a union energy mesh from the original energy meshes for all the isotopes in the problem. The macroscopic total cross sections are computed on the union mesh and used to thin the union mesh in such a manner that the macroscopic total cross section can be linearly interpolated according to a specific tolerance. Another constraint that adds more points to the mesh is that the maximum interval width between two successive points should be less than one-third of the maximum lethargy gain of the neutron due to elastic scattering from the heaviest isotope. After unionizing, thinning and adding additional points, the final energy mesh is used for the slowing-down calculation.

The rest of this section describes the treatment of the in-scatter source with the problem-dependent mesh. Starting from Eq. (2), the exponential quantity is written in terms of energy to avoid the exponential calculation

$$\sum_i \Sigma_{t,i}(u)\phi(u) = \sum_i \int_{u-\varepsilon_i}^{u} \frac{E\Sigma_{s,i}(u')}{E'(1-\alpha_i)}\phi(u')du' \tag{9}$$

Equation (9) is satisfied at each point on the problem-dependent mesh,

$$\sum_i \Sigma_{t,i}(u_n)\phi_n = \sum_i \int_{u_n-\varepsilon_i}^{u_n} \frac{E_n\Sigma_{s,i}(u')}{E'(1-\alpha_i)}\phi(u')du' \tag{10}$$

Define *m* as the number of lethargy points that a neutron scattering from nuclide *i* will traverse from lethargy $u_n - \varepsilon_i$ to u_n (not including u_n), so that the integral in Eq. (10) can be split into *m* sub-integrals plus an extra term integrated from $u_n - \varepsilon_i$ to u_{n-m}

$$\sum_i \Sigma_{t,i}(u_n)\phi_n = \sum_i \left[\sum_{j=1}^{m} \int_{u_{n-j}}^{u_{n-j+1}} \frac{E_n\Sigma_{s,i}(u')}{E'(1-\alpha_i)}\phi(u')du' + \int_{u_n-\varepsilon_i}^{u_{n-m}} \frac{E_n\Sigma_{s,i}(u')}{E'(1-\alpha_i)}\phi(u')du' \right] \tag{11}$$

These integrals except the last one are evaluated with trapezoidal rule,

$$\begin{aligned}
\sum_i \Sigma_{t,i}(u_n)\phi_n &= \sum_i \frac{E_n}{2(1-\alpha_i)} \left[\sum_{j=1}^{m} \Delta u_{n-j} \left(\frac{\Sigma_{s,i}(u_{n-j+1})\phi_{n-j+1}}{E_{n-j+1}} + \frac{\Sigma_{s,i}(u_{n-j})\phi_{n-j}}{E_{n-j}} \right) + \Delta S_{i,n,m} \right] \\
&= \Sigma_{s,nn}\phi_n + \Sigma_{s,n'n}\phi_{n-1} + \sum_i \frac{E_n}{2(1-\alpha_i)} \left[\sum_{j=2}^{m} \Delta u_{n-j} \left(\frac{\Sigma_{s,i}(u_{n-j+1})\phi_{n-j+1}}{E_{n-j+1}} + \frac{\Sigma_{s,i}(u_{n-j})\phi_{n-j}}{E_{n-j}} \right) + \Delta S_{i,n,m} \right]
\end{aligned} \tag{12}$$

where $\Delta u_{n-j} = u_{n-j+1} - u_{n-j}$, $\Sigma_{s,nn} = \sum_i \frac{1}{2(1-\alpha_i)} \Delta u_{n-1}\Sigma_{s,i}(u_n)$,

$\Sigma_{s,n'n} = \sum_i \frac{E_n}{2(1-\alpha_i)E_{n-1}} \Delta u_{n-1}\Sigma_{s,i}(u_{n-1})$, and $\Delta S_{i,n,m} = \int_{u_n-\varepsilon_i}^{u_{n-m}} \frac{\Sigma_{s,i}(u')}{E'(1-\alpha_i)}\phi(u')du'$.

Since the maximum lethargy gain for scattering off the heaviest nuclide is always greater than the maximum lethargy mesh spacing ($m \geq 1$), the interior term $\Sigma_{s,nn}\phi_n$ always exists and can be rearranged,

$$\begin{aligned}
&\left(\sum_i \Sigma_{t,i}(u_n) - \Sigma_{s,nn} \right)\phi_n = \Sigma_{s,n'n}\phi_{n-1} + \\
&E_n \sum_i \frac{1}{2(1-\alpha_i)} \left[\sum_{j=2}^{m} \Delta u_{n-j} \left(\frac{\Sigma_{s,i}(u_{n-j+1})\phi_{n-j+1}}{E_{n-j+1}} + \frac{\Sigma_{s,i}(u_{n-j})\phi_{n-j}}{E_{n-j}} \right) + \Delta S_{i,n,m} \right]
\end{aligned} \tag{13}$$

CASL-U-2015-0007-000

Even for heavy nuclides such as uranium and plutonium, the number m can be a few hundred. To avoid the time-consuming summation over j for every energy point n, a cumulative term for each isotope i is defined to facilitate the summation [1],

$$C_{i,n} = \frac{1}{2(1-\alpha_i)} \sum_{j=1}^{n-1} \Delta u_j \left(\frac{\Sigma_{s,i,j+1}\phi_{j+1}}{E_{j+1}} + \frac{\Sigma_{s,i,j}\phi_j}{E_j} \right) \tag{14}$$

Thus, the summation term over j on the right-hand side of Eq. (13) can be replaced by subtraction of two cumulative terms:

$$\frac{1}{2(1-\alpha_i)} \sum_{j=2}^{m} \Delta u_{n-j} \left(\frac{\Sigma_{s,i}(u_{n-j+1})\phi_{n-j+1}}{E_{n-j+1}} + \frac{\Sigma_{s,i}(u_{n-j})\phi_{n-j}}{E_{n-j}} \right) = C_{i,n-1} - C_{i,n-m} \tag{15}$$

The extra term $\Delta S_{i,n,m}$ can be interpolated from $C_{i,n-m} - C_{i,n-m-1}$ by the lethargy difference. To sum up, three independent terms need to be evaluated for each lethargy point n, i.e., $\Sigma_{s,nn}$, $\Sigma_{s,n'n}$ and $\frac{1}{2(1-\alpha_i)} \Delta u_{n-1} \left(\frac{\Sigma_{s,i,n}\phi_n}{E_n} + \frac{\Sigma_{s,i,n-1}\phi_{n-1}}{E_{n-1}} \right)$. Note the last value is done for each isotope and is evaluated when the calculation of ϕ_n is complete. It is accumulated by Eq. (14) and will be used by the next lethargy point $n+1$.

Condensation of multigroup effective cross sections for the problem-dependent mesh needs careful consideration. As the mesh thinning is based on a specified tolerance for linear interpolation of the macroscopic total cross section for the whole material, there should be some cross section variation on energy existing in the original cross section mesh of an isotope, however, missing in the thinned flux mesh. To retrieve the cross section subtleties of each isotope, the original mesh of the isotope and the thinned flux mesh are unionized as the final mesh for the integration of effective cross sections. The flux interpolation in the union mesh is performed by the total reaction rate ($\Sigma_t\phi_t$) instead of flux itself, because the reaction rates versus energy is much smoother than the flux.

2.3. RI Interpolation of Single Resonant Isotope

The RIF model requires two sets of self-shielded multigroup cross sections created for every resonance isotope in the fuel. One set is created with a flux spectrum calculated by considering the entire fuel mixture of resonance isotopes. This spectrum has to be solved from the slowing-down Equation (7). The other set is created with a flux spectrum generated by isolating a single resonance isotope from all other absorbers in the fuel mixture. This set of effective cross sections can be efficiently interpolated from homogeneous RI tables rather than being expensively solved on the fly. In this sense, the slowing-down solver is performed only once for each mixture, which significantly reduces the computation time. Detailed procedures of generating the homogeneous RI tables as well as IR factors can be found in Ref. [11].

Usually the IR factors are only calculated against the resonances of ^{238}U, which is the dominant isotope in PWR fuels. However, in our application, every resonance isotope is isolated when the non-interfered cross sections are being calculated. Thus, each isotope should have *m* sets of IR factors, where *m* is the number of resonance isotopes. Typically the total number of groups *g* is around a hundred, hence the corresponding number of IR factors read into the program will be $g \times m \times n$, where *n* is the number of isotopes in the problem. Consequently, the number of IR factors is in the same order as the number of point-wise cross sections of an isotope, which will not impose a significant memory increase with this method.

3. Calculation and Results

3.1. Cross Section Library and RI Tables

The homogeneous slowing-down solver was firstly developed in compatibility with SCALE 6.1 code systems [17] using CE libraries generated by AMPX [18]. Also the 60 group multigroup library provided by ORNL was processed by AMPX. Since it is desirable to perform the verifications with a general Monte Carlo code, such as MCNP5 [19], a set of multigroup resonance data that are consistent with the Monte Carlo calculations are needed to assess the significance of interference effect, eliminating other possible issues that might result in discrepancies in the resonance cross sections, such as treatment of the unresolved energy range and up-scattering considerations in the lower energy range. Fig. 1 depicts the overall picture for the cross section data flow for the entire calculational system. The raw cross section data are based on ENDF/B-VII.0 [20], although NJOY [21] and AMPX processing systems are performed for different purposes. The *heterogeneous* RI tables generated by MCNP correspond to a variety of background cross sections for a 2-D pin cell problem and were done by varying the configurations of the pin cell geometry and compositions of the materials [22]. One million neutron histories from a fixed neutron source for each case are simulated to achieve 1% standard deviations for tallies of effective cross sections. These RI tables are different from the *homogenous* ones mentioned in Section 2.3 which are processed by homogenizing hydrogen with each resonance isotope. Thus the RI tables in the 60 group multigroup library have been replaced by the MCNP generated RI tables for the purpose of consistent comparisons.

CASL-U-2015-0007-000

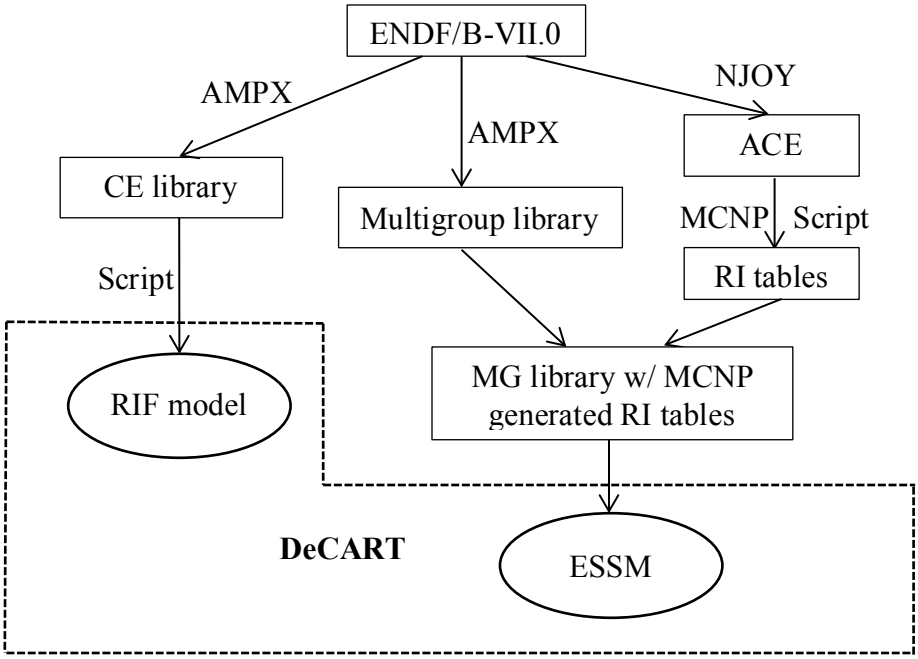

Figure 1. Cross section data flow for the resonance calculation

3.2. Verification and Results

In this section, three pin cell cases are analyzed by the version of DeCART that includes ESSM and the RIF model, and are compared with MCNP5 calculations. Table 1 shows the physical parameters of the pin-cell configurations. The depleted UO_2 fuel (Case 3) contains 87 isotopes, including 23 resonance isotopes.

Table 1 Parameters of the pin-cell cases

Case	Material	Geometry	Temperature
1	UO_2 (5.0 w/o ^{235}U)	Pitch = 1.26cm Fuel radius= 0.4069cm Cladding inner = 0.418cm Cladding outer = 0.475cm	600K everywhere
2	MOX (1.2 w/o ^{235}U, 4.0 w/o ^{239}Pu)		
3	Depleted UO_2 (25 MWd/kgU)		

The DeCART code includes an option to use Bondarenko iteration for the treatment of resonance interference. This option is turned off when the present RIF model is applied. The effective cross sections are compared between Bondarenko iteration and RIF model. To avoid cluttering the results, the case with no interference is not included in the following plots because the results are close to the results obtained by Bondarenko iteration. Therefore, the differences between the RIF model and Bondarenko iteration indicate the strength of the interference effect. Figures 2-4 provide a comparison of the self-shielded cross sections for Case 1. Since ^{238}U is the most

abundant resonance isotope which dominates the final spectrum of the fuel, the interference effect from ^{235}U to ^{238}U is marginal, essentially submerged in the statistical noise of the RI tables. On the contrary, the resonance peaks of ^{238}U strongly interfere with the effective absorption and fission rates in ^{235}U and the RIF model gives an excellent correction on the effective cross sections for ^{235}U. As for Case 2, Figures 5-6 present the effective cross sections of ^{238}U and ^{239}Pu, omitting ^{235}U because the results are very similar to the UO_2 case. Due to the combination effect of ^{235}U and ^{239}Pu resonances, RIF correction of ^{238}U is more noticeable than the UO_2 case. In all, the effective cross sections corrected by RIF model are in good agreement with MCNP5 for both fuel types, except for a single group of ^{239}Pu absorption whose bigger error is probably due to the statistic noise of the RI tables generated by MCNP5.

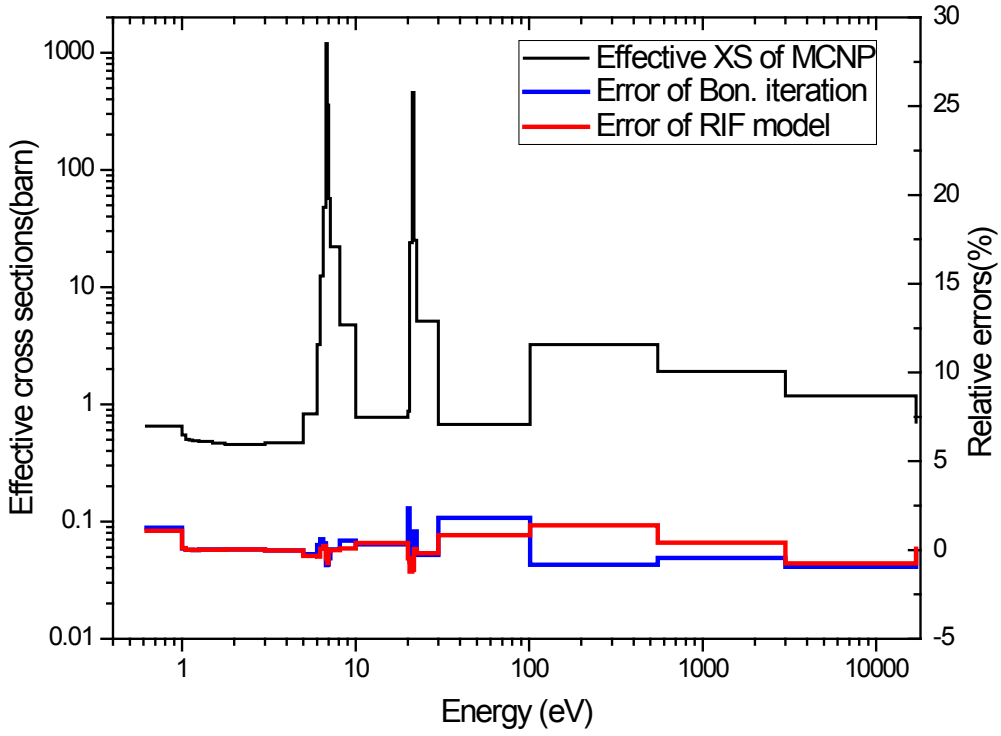

Figure 2. Multi-group effective absorption of ^{238}U in UO_2 fuel

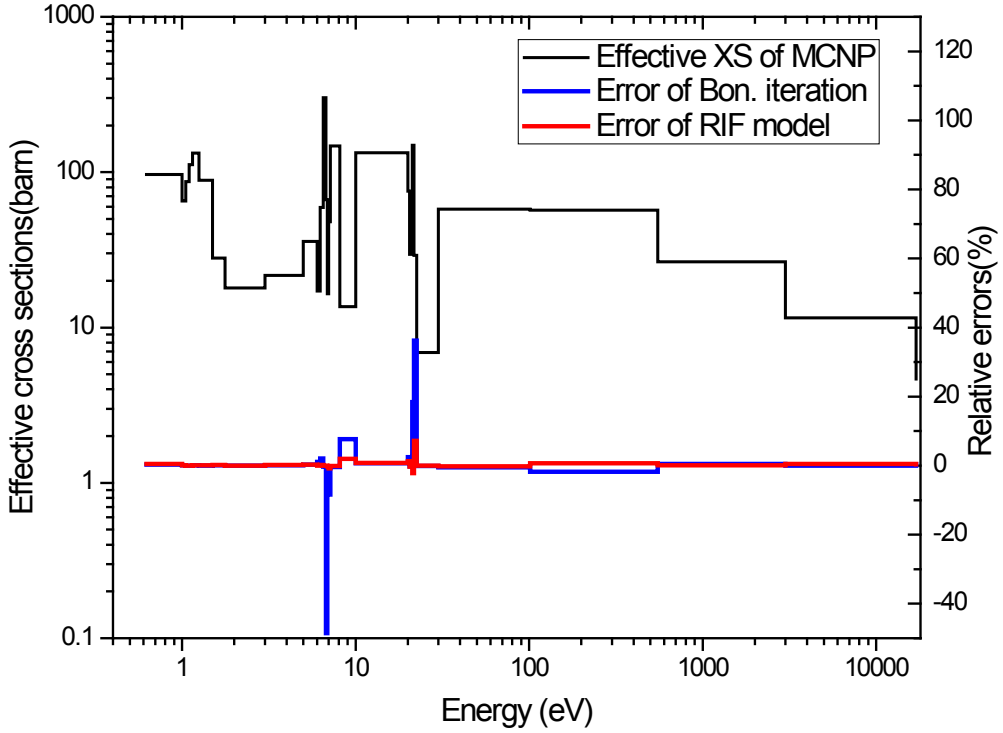

Figure 3. Multi-group effective absorption of ^{235}U in UO_2 fuel

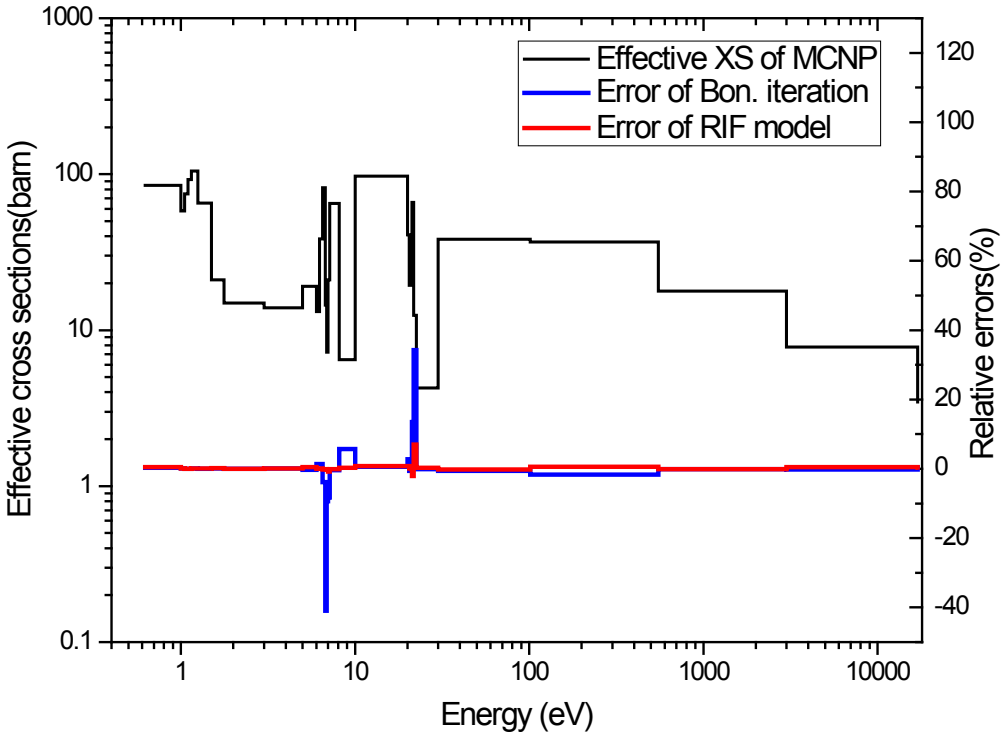

Figure 4. Multi-group effective fission of ^{235}U in UO_2 fuel

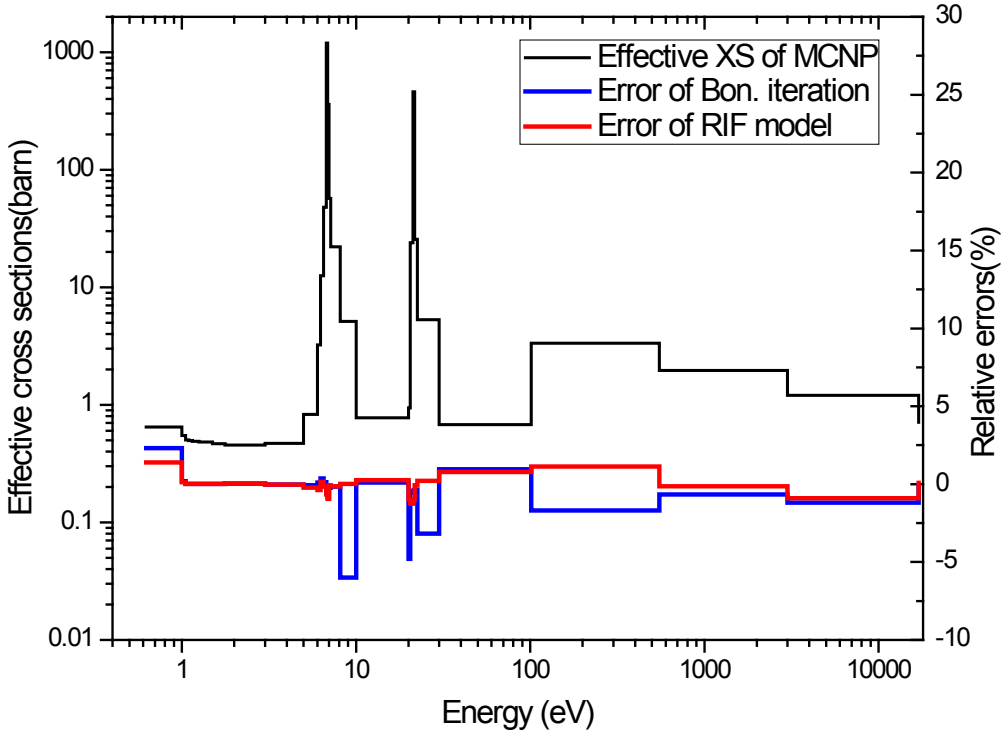

Figure 5. Multi-group effective absorption of ^{238}U in MOX fuel

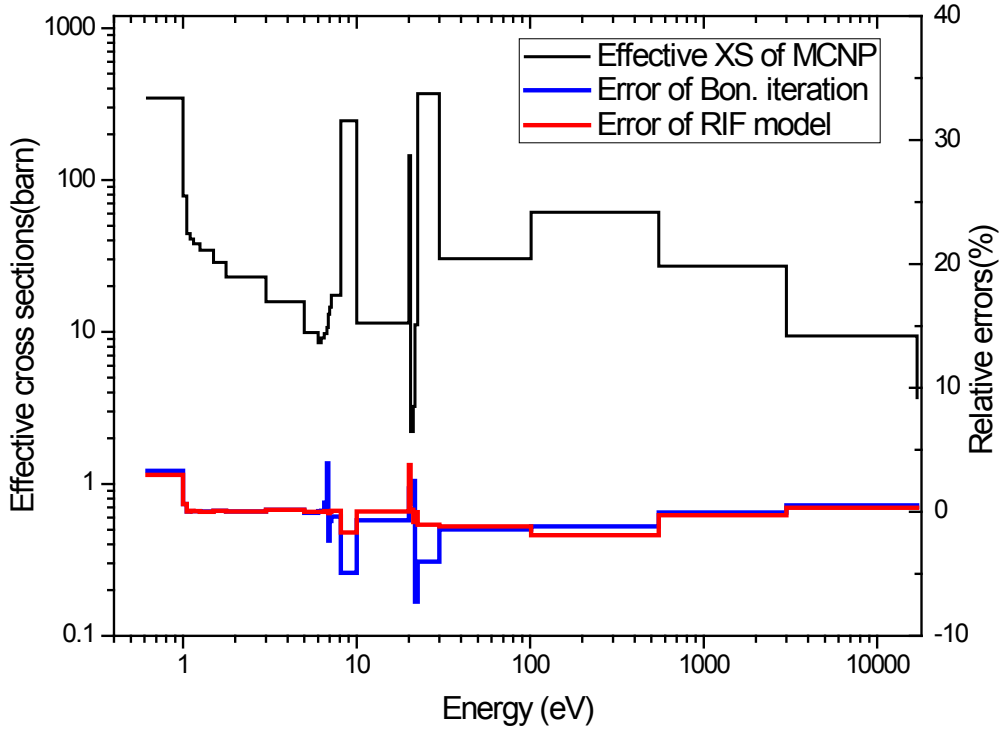

Figure 6. Multi-group effective absorption of ^{239}Pu in MOX fuel

CASL-U-2015-0007-000

The effective cross sections obtained in Case 3 are also in good agreement with the Monte Carlo solutions. To keep it brief, we just present the multiplication factors in Table 2. The RIF model always provides better multiplication factors for the three cases. The relatively larger discrepancy of eigenvalue for Case 3 is explained in Ref. [23]. ESSM considers the absorption of resonance isotopes as a whole material when solving the FSP equations. This treatment underestimates the equivalence cross sections as compared to singling out isotope or isotope category and hence overestimates the eigenvalue especially when the number of absorbers is large for the depleted cases.

Table 2 Comparisons of multiplication factors

Case	MCNP5	DeCART Bon.	$\Delta\rho$(pcm)	DeCART RIF	$\Delta\rho$(pcm)
1	1.38861(0.00016)	1.39009	+77	1.38906	+23
2	1.41062(0.00016)	1.41241	+90	1.40957	-53
3	1.01275(0.00017)	1.01580	+296	1.01487	+206

A comparison of the execution time and memory demand for the RIF method is given in Table 3. Comparisons of the execution time for the three cases indicate that the time for solving FSP of ESSM is not dependent on the number of resonance isotopes because FSP is solved only once considering all resonance isotopes as a whole absorber to obtain the equivalence cross sections. Additional time spent on RIF correction is not significant for the three cases because the slowing-down solver is performed only once for the mixture, with each isolating isotope using table interpolation. Since the point-wise cross sections are required for RIF correction, the memory demand has been increased, especially in Case 3 where the total number of isotopes is large in the problem. After all, the memory demand for RIF correction is still acceptable because of using the problem-dependent energy mesh.

Table 3 Comparisons of computational resources

Case	DeCART-Bondarenko iteration			DeCART-RIF		
	Total time(s)[a]	Res. time(s)[b]	Memory(MB)	Total time(s)	Res. time(s)	Memory(MB)
1	14.5	1.1	86	17.2	1.2	130
2	16.9	1.1	86	17.7	1.2	143
3	34.1	1.2	87	29.1	2.4 (12.4[c])	464 (1840[d])

[a]. Total computation time of the eigenvalue problem including everything. The convergence rate of eigenvalues may vary due to the changes of effective cross sections. This is the reason why the total time applying RIF model is even faster than Bondarenko iteration for Case 3.
[b]. Time spent on resonance calculation, i.e. solving FSP and treating resonance interference.
[c]. Time if solving slowing-down equation for both mixture and isolating resonance isotopes.
[d]. Memory use if employing the equal-lethargy energy mesh (1 million energy points).

CASL-U-2015-0007-000

4. Conclusions

In order to model the resonance interference effect, an improved RIF method is developed, consisting of an optimized homogeneous slowing-down solver to calculate the effective cross sections with and without interference. ESSM is chosen to be the solver of heterogeneous resonance self-shielding and implemented into the transport code DeCART. The whole system can provide more accurate self-shielded cross sections for UO_2 and MOX fuels compared to the crude treatment of Bondarenko iteration which is almost the same as no interference treatment. The multiplication factors are improved for all the test cases with the improved RIF model.

Two features of the homogeneous slowing-down solver have proven to be very useful for computational efficiency. The homogeneous RI tables are generated in such a way to yield the self-shielded cross section for an isolated resonance isotope, avoiding the need to solve the slowing-down equation. This ensures that the RIF model does not significantly increase the computing time of resonance calculation even for a problem with depletion. A simplified form of a problem-dependent energy mesh is developed for the homogeneous slowing-down solver to minimize memory demand. The RIF method can be easily extended for parallel clusters because the treatment of resonance materials in different regions do not depend on each other.

ACKNOWLEDGMENTS

This research was supported by the Consortium for Advanced Simulation of Light Water Reactors (http://www.casl.gov), an Energy Innovation Hub (http://www.energy.gov/hubs) for Modeling and Simulation of Nuclear Reactors under U.S. Department of Energy Contract No. DE-AC05-00OR22725.

REFERENCES

1. M. L. Williams and M. Asgari, "Computation of Continuous-Energy Neutron Spectra with Discrete Ordinates Transport Theory," *Nucl. Sci. Eng*., **121**, pp.173-201 (1974).
2. F. Leszczynski, "Neutron Resonance Treatment with Details in Space and Energy for Pin Cells and Rod Clusters," *Ann. Nucl. Energy*, **14**, pp.589-601 (1987).
3. R. J. J. Stamm'ler and M. J. Abbate, *Methods of Steady-state Reactor Physics in Nuclear Design*, Academic Press, London (1983).
4. I. I. Bondarenko, et al., *Group Constants for Nuclear Reactor Calculations*, Consultants Bureau, New York (1964).
5. D. E. Cullen, "Application of the Probability Table Method to Multigroup Calculations of Neutron Transport," *Nucl. Sci. Eng*. **55**, 387 (1974).
6. S. G. Hong and K. S. Kim, "Iterative Resonance Self-Shielding Methods Using Resonance Integral Table in Heterogeneous Transport Lattice Calculations," *Ann. Nucl. Eng.*, **38**, pp.32-43 (2011).
7. M. L. Williams and K. S. Kim, "The Embedded Self-shielding Method," *PHYSOR-2012*, Knoxville, TN, April 15-20, (2012).
8. J. R. Askew, F. J. Fayers, and P. B. Kemshell, "A General Description of the Lattice Code WIMS," *J. British Nucl. Energy Soc.*, **5**, pp.564-585 (1966).

9. M. L. Williams, "Correction of Multigroup Cross Sections for Resolved Resonance Interference in Mixed Absorbers," *Nucl. Sci. Eng*., **83**, pp.37-49 (1983).
10. K. S. Kim and S. G. Hong, "A New Procedure to Generate Resonance Integral Table with an Explicit Resonance Interference for Transport Lattice Codes," *Ann. Nucl. Energy*, **38**, pp.118-127 (2011).
11. Z. Gao, Y. Xu, and T. J. Downar, "The Treatment of Resonance Interference Effects in the Subgroup Method," *Ann. Nucl. Energy*, **38,** pp. 995-1103 (2011).
12. E. Wehlage, "Modeling Resonance Interference Effects in the Lattice Physics Code LANCER02," *Mathematics and Computation, Supercomputing, Reactor Physics and Nuclear and Biological Applications*, Avignon, France, Sep. 12-15 (2005).
13. K. S. Kim and M. L. Williams, "Preliminary Assessment of Resonance Interference Consideration by Using 0-D Slowing Down Calculation in the Embedded Self-Shielding Method," ANS Winter Meeting, San Diego, CA, Nov. 11-15 (2012).
14. K. S. Kim and M. L. Williams, "Resonance Interference Corrections for Embedded Self-Shielding and Subgroup Methods Using Pointwise Fluxes," to be published.
15. H. G. Joo, et al., "Methods and Performance of a Three-Dimensional Whole-Core Transport Code DeCART," *Proc. PHYSOR-2004*, Chicago, IL, April 25-29 (2004).
16. R. Goldstein and E. R. Cohen, "Theory of resonance absorption of neutrons," *Nucl. Sci. Eng*., **13**, pp.132-140 (1962).
17. S. M. Bowman, "SCALE 6: Comprehensive Nuclear Safety Analysis Code System," *Nucl. Technol*. **174**, pp.126-148 (2011).
18. M. E. Dunn and N. M. Greene, "AMPX-2000: A Cross-Section Processing System for Generating Nuclear Data for Criticality Safety Applications," *Trans. Am. Nucl. Soc*. **86**, 118-119 (2002).
19. X-5 Monte Carlo Team, "MCNP-A General Monte Carlo N-Particle Transport Code, Version 5", Los Alamos National Laboratory, (2003).
20. M. B. Chadwick, et al., "ENDF/B-VII.0: Next Generation Evaluated Nuclear Data Library for Nuclear Science and Technology," *Nucl. Data Sheets*, 107, pp.2931-3060 (2006).
21. R. E. MacFarlane and D. W. Muir, "NJOY99.0 code system for producing pointwise and multigroup neutron and photon cross sections from ENDF/B Data," Report PSR-480/NJOY99.0, Los Alamos National Laboratory, New Mexico (2000).
22. H.G. Joo, et al., "Subgroup weight generation based on shielded pin-cell cross section conservation," *Ann. Nucl. Energy* **36**, pp.859-868 (2009).
23. Y. Liu, et al., "Resonance Self-shielding Methodology in MPACT," submitted to M&C 2013, Sun Valley, Idaho, USA.